6616 *Macromolecules* **2010**, *43*, 6616–6624
DOI: 10.1021/ma100776d

Macromolecules
ARTICLE

Multifunctional Polymeric Scaffolds for Enhancement of PARACEST Contrast Sensitivity and Performance: Effects of Random Copolymer Variations

Yunkou Wu,[†] Piyu Zhao,[†] Garry E. Kiefer,[†,‡] and A. Dean Sherry*[,†,§]

[†]*Department of Chemistry, University of Texas at Dallas, P.O. Box 830668, Richardson, Texas 75083,* [‡]*Macrocyclics, Inc., 1309 Record Crossing, Dallas, Texas 75235, and* [§]*Advanced Imaging Research Center, The University of Texas Southwestern Medical Center, 5323 Harry Hines Boulevard, Dallas, Texas 75390*

Received April 9, 2010; Revised Manuscript Received July 1, 2010

ABSTRACT: A DOTA (1,4,7,10-tetraazacyclododecane-*N*,*N*′,*N*″,*N*‴-tetraacetic acid) tetraamide ligand having a single acrylamide side chain (M1) was copolymerized with either 2-methylacrylic acid (MAA), 2-(acryloylamino)-2-methyl-1-propanesulfonic acid (AMPS), or *N*-isopropylacrylamide (NIPAM) to create a series of linear random copolymers using classical free radical chain polymerization chemistry. The metal ion binding properties of hydrolyzed M1 were investigated by pH potentiometry and the europium(III) complexes of the resulting heteropolymers were evaluated as PARACEST imaging agents. All polymeric agents were found to possess similar intermediate-to-slow water exchange and CEST characteristics as the parent EuDOTA-tetraamide monomer. Consistent with basic multiplexing principles, the highest molecular weight polymer, Eu-DMAA 3.1, also showed the highest CEST sensitivity with a detection limit of $20 \pm 2\ \mu$M. The second arylamide component gave polymers with widely different chemical characteristics and CEST properties. In particular, the Eu-DNIPAM 4.0 and Eu-DMAA 4.1 polymers displayed different solubility characteristics as a function of pH or temperature which, in turn, affected the water exchange and CEST properties of the corresponding agents. It was concluded that introduction of hydrophobic groups into the polymer backbone reduces solvent accessibility to the Eu^{3+} component, effectively slowing water exchange between the inner-sphere water coordination position at each Eu^{3+} center with bulk water. The CEST properties of the heteropolymers when dissolved in plasma suggest that the more hydrophobic characteristics of these polymers could be advantageous for *in vivo* applications.

Introduction

Magnetic resonance imaging (MRI) is one of the most important noninvasive clinical tools for anatomical imaging. A critical component in the advancement of MRI in clinical medicine was the codevelopment of gadolinium(III) contrast agents for altering image contrast. Traditional Gd^{3+}-based chelates that function by shortening bulk water proton relaxation times (T_1, T_2, or T_2*) have been the cornerstone of clinical MRI contrast agents for the past two decades.[1,2] These agents are most often used as general perfusion agents typically requiring injection at high concentration to be effective. A major research goal over the past few years has been the design and development of second generation agents that report specific biological or physiological information about tissue. Furthermore, increasing the sensitivity of MR contrast agents has become an important goal for molecular imaging applications.[3]

Toward this end, the recent development of a new class of MR contrast agents based on chemical exchange saturation transfer (CEST) has attracted considerable interest. Paramagnetic molecules that provide changes in image contrast via the CEST effect have been coined PARACEST agents.[4] Unlike Gd^{3+}-based agents that rely on rapid water exchange between metal ion bound water and bulk solvent, PARACEST agents require moderate-to-slow water exchange rates for optimal performance. To generate a CEST effect, the slowly exchanging bound protons on the agent are first saturated using a frequency-selective radio frequency (rf) pulse, and those protons subsequently undergo chemical exchange with bulk water protons to attenuate the bulk water proton signal.[4,5] As this new mechanism is highly sensitive to the rate at which these protons undergo chemical exchange, it is relatively easy to find systems that respond to their local tissue environment by altering this chemical exchange rate and thereby the intensity of the tissue water signal. PARACEST agents offer one substantial advantage over diamagnetic systems in that the exchanging proton site is typically frequency shifted well away from the tissue water signal, and this permits more selective rf saturation at this site without inadvertent partial saturation of the bulk water signal itself.[6,7] Consequently, a number of newer PARACEST agents have been reported that respond to physiological changes such as pH,[8−11] temperature,[10,12,13] Zn^{2+},[14] glucose,[15−17] lactate,[18] nitric oxide,[19] phosphate esters,[20] and enzyme activities.[21−23]

A major limitation of PARACEST agents is their inherently low contrast sensitivity, typically requiring 1−10 mM agent concentrations for detection. The contrast sensitivity of low molecular weight Gd^{3+}-based agents can be significantly improved by either covalent or noncovalent coupling of multiple Gd^{3+} complexes to a macromolecular scaffold such as dendrimers,[24] polymers,[25] or nanoparticles.[26] This approach not only enhances the molecular relaxivity and the sensitivity of the agent and but also results in prolonged blood circulation times and hence provides a longer imaging time window.[25] Similarly, the sensitivity of CEST agents can be significantly amplified by multiple incorporations of exchangeable protons within macromolecular systems. This was first demonstrated by van Zijl and co-workers in various diamagnetic macromolecular systems including poly(amino acids),[27] single-stranded RNA,[5] and glycogen,[5] and later this strategy was extended by Aime and co-workers to paramagnetic macromolecular

*Corresponding author. E-mail: sherry@utdallas.edu, dean.sherry@utsouthwestern.edu.

 Published on Web 07/21/2010

Chart 1. Structures of Monomers M1 and M2 and Homopolymer H1

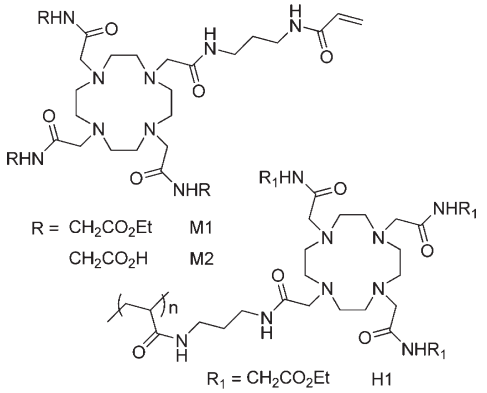

Chart 2. Chemical Components of Copolymers Prepared in This Work

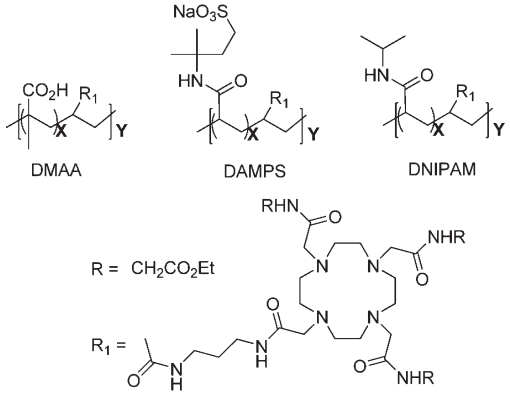

systems by exploiting the formation of a noncovalent supramolecular adduct between a paramagnetic shift reagent $[TmHdotp]^{4-}$ and a macromolecular substrate polyarginine.[28] Furthermore, multiple pH-sensitive PARACEST agents have been introduced into dendrimers for pH sensing.[11]

We recently reported linear PARACEST homopolymers prepared by free radical polymerization of a DOTA (1,4,7,10-tetraazacyclododecane-*N*,*N*′,*N*″,*N*‴-tetraacetic acid) tetraamide monomer, M1 (Chart 1), and demonstrated that the CEST detection limit could be lowered to the micromolar range for relatively small homopolymers (10−18 repeating units).[29] These results stimulated the present investigation of PARACEST heteropolymers consisting of variable copolymer side chains to introduce more chemical functionality into these highly sensitive CEST imaging agents (Chart 2). The current study was aimed at addressing whether one could further increase the molecular size of PARACEST polymers by introducing non-CEST acrylamide units as spacers between the Eu^{3+}-based CEST units while retaining the same CEST properties per Eu^{3+} center. Introduction of other chemical groups between the Eu^{3+} centers could also change the overall chemical properties of the homopolymer compared to the heteropolymer. To test this, we introduced acrylamide spacers composed of either methacrylic acid (MAA), 2-(acryloylamino)-2-methyl-1-propanesulfonic acid (AMPS), or *N*-isopropylacrylamide (NIPAM) and evaluated the sizes and other physical and CEST properties of the resulting homopolymers.

Results and Discussion

A. Equilibrium Studies. Thermodynamic and kinetic stability data on potential new imaging agents are fundamentally important for evaluating whether they may be suitable for use *in vivo*.[1] Given that ethyl ester groups of DOTA-tetraamide ligand were found to hydrolyze slowly in aqueous solution,[30] equilibrium measurements were performed only on the free acid monomer, M2 (Chart 1). The protonation constants of M2 as determined by pH potentiometry are compared with those of DOTA-$(gly)_4$[31] in Table S1. The number of protonation constants found for M2 is consistent with its structure. The first two protonation steps, $Log K_1^H$ and $Log K_2^H$, and the last three ($Log K_3^H$ to $Log K_5^H$) were numerically similar to many other DOTA-tetraamide derivatives reported previously,[31] reflecting protonation of macrocyclic ring amines and carboxylate groups, respectively. Equilibruim between M2 and different divalent transition metal ions was achieved rapidly enough to allow direct potentiometric titrations of those samples (Table 1). The rate of complex formation between M2 and Eu^{3+}, however, was rather slow so this value was obtained by the "out of cell" technique[31] from pH data on samples equilibrated for several weeks in separate vials. Like DOTA-$(gly)_4$ (Table S2), the three carboxylate groups in M2 are not involved in coordination to these metal ions so they can accept protons to form different MLH_i species. The potentiometric data for M2 and Mg^{2+} was easily described by formation of ML-type complexes only while those with the other divalent metal ions required the inclusion of protonated species in the equilibrium model. The stability constant ($Log K_{ML}$) of CaL was found to be about 6 orders of magnitude higher than MgL while the ZnL and CuL were even higher, as expected. Three protonated species, MLH_1, MLH_2, and MLH_3, were found for the CuL and ZnL systems in addition to one deprotonated species MLH_{-1} at pH values above which the complexes are fully formed. The $Log K_{ML}$ of EuL is close to those of ZnL and CuL, but only the ML and MLH_1 species were observed in this case.

B. Copolymer Synthesis and Characterization. Free-radical polymerization is one of most widely used methods for the preparation of copolymers with different chemical repeating units randomly arranged within the polymer chain.[32] Compared to the preparation of the homopolymer (H1), one might anticipate that the degree of copolymerization would be greater in these heteropolymers since less bulky co-monomers may reduce steric or electrostatic interactions between the macrocyclic monomer subunits during the chain propagation process. In addition, the resulting copolymers could have significantly different chemical characteristics (charge, solubility, rigidity) compared to the homopolymers. For example, poly(methacrylic acid) (PMAA) and poly(*N*-isopropylacrylamide) (PNIPAM) polymers are often used as pH and thermoresponsive smart polymers, respectively, that can be physically blended with or chemically conjugated to biomolecules to yield a large family of polymer−biomolecule systems that respond to biological, physical, and chemical stimuli.[33] Thus, introduction of the hydrophilic methacrylic acid (MAA) or 2-(acryloylamino)-2-methyl-1-propanesulfonic acid (AMPS) monomer or the hydrophobic *N*-isopropylacrylamide (NIPAM) monomer into the polymer should change the physical properties of the resulting polymers, and this, in turn, could alter the water exchange and CEST imaging characteristics of these systems as well.

Copolymerization of M1 with MAA or AMPS was conducted in water using azo-bis(4-cyanovaleric acid) as initiator. The amount of M1 and initiator was held constant in each copolymerization reaction while the ratio of MAA or AMPS monomer relative to M1 was varied from 1/3 to 9 mol equiv. Given the acidic properties of the MAA and AMPS monomers, the reactions were also performed at different pH values (Tables 2 and 3). Copolymerization of M1 with NIPAM was performed in DMF (Table 4) because of the lower critical solution temperature (LCST) behavior of NIPAM involved polymers.[33] All reactions were maintained at 70 °C for 24 h under a N_2 atmosphere. The resulting water-soluble copolymers were purified by dialysis using 3000 MW cutoff dialysis tubing.

Table 1. Stability Constants (log *K*) of M2 Complexes with Some Metal Ions at 1.0 M KCl and 25 °C

ligand	species	Ca^{2+}	Mg^{2+}	Cu^{2+}	Zn^{2+}	Eu^{3+} [a]
M2	MLH_3			3.02 ± 0.03	3.16 ± 0.02	
	MLH_2			3.29 ± 0.02	3.12 ± 0.03	
	MLH_1	4.31 ± 0.06		4.46 ± 0.03	4.38 ± 0.02	3.50 ± 0.01
	ML	9.82 ± 0.04	3.81 ± 0.08	14.99 ± 0.03	12.77 ± 0.02	13.00 ± 0.01
	MLH_{-1}			9.39 ± 0.06	9.31 ± 0.06	

[a] Measured using the "out-of-cell" technique.[31]

Table 2. Copolymerization[a] and Characterization Data for DMAA Copolymers

copolymer	feed composition MAA/M1	pH	X [b]	M_n (Da)	Y [c]
DMAA 1.1	0.33	6	0.6	18 500	22.6
DMAA 2.0	1	4.5	1.3	13 000	14.8
DMAA 2.1	1	6	1.2	28 900	33.1
DMAA 3.0	3	4	2.7	36 700	36.6
DMAA 3.1	3	6	2.6	58 500	58.9
DMAA 4.1	9	6	8.2	30 100	12.7

[a] 120 mg of M1, 12 mg of initiator, and 4 mL of water were used in each copolymerization. [b] Copolymer composition MAA/M1 (based on NMR). [c] Degree of copolymerization (as defined by $[(MAA)_X{-}M1]_Y$ in Chart 2).

Table 3. Copolymerization[a] and Characterization Data for DAMPS Copolymers

copolymer	feed composition AMPS/M1	pH	X [b]	M_n (Da)	Y [c]
DAMPS 1.1	0.33	6	0.7	11 200	12.0
DAMPS 2.0	1	5	1.4	16 400	14.8
DAMPS 2.1	1	6	1.4	18 200	16.6
DAMPS 3.0	3	1.5	23.0	36 700	5.8
DAMPS 3.1	3	6	3.2	30 900	20.1
DAMPS 4.1[d]	9	6	8.5		

[a] 120 mg of M1, 12 mg of initiator, and 4 mL of water were used in each copolymerization. [b] Copolymer composition AMPS/M1 (based on NMR). [c] Degree of copolymerization (as defined by $[(AMPS)_X{-}M1]_Y$ in Chart 2). [d] Insoluble in DMF.

Table 4. Copolymerization[a] and Characterization Data for DNIPAM Copolymers

copolymer	feed composition NIPAM/M1	X [b]	M_n (Da)	Y [c]
DNIPAM 3.0	3	3.2	2100	1.9
DNIPAM 4.0	9	9.1	5600	3.1

[a] 120 mg of M1, 12 mg of initiator, and 4 mL of DMF were used in each copolymerization. [b] Copolymer composition NIPAM/M1 (as determined by NMR). [c] Degree of copolymerization (as defined by $[(NIPAM)_X{-}M1]_Y$ in Chart 2).

Figure 1 compares ^{1}H NMR spectra of the monomer, the homopolymer H1, and the heteropolymer DMAA 2.1. The assignments of the copolymer spectrum were made by comparison with the NMR spectra of monomer M1 and homopolymer H1. The methyl proton resonance labeled peak 1 is easily assigned to the three ethyl ester groups of the macrocyclic component while the upfield methyl resonance 2 reflects the MAA component. The absence of peak 3 in copolymer samples indicates the polymer is free of monomer. The ratio of MAA to macrocyclic component M1 (X) in each DMAA copolymer is then given by eq 1. A value of $X = 1.2$ derived from the NMR spectrum of this particular DMAA 2.1 sample indicates that the copolymer composition is comparable to the original feed composition.

$$X = \frac{\text{area (peak 2)} \times 9}{\text{area (peak 1)} \times 3} \quad (1)$$

However, if one examines values found for X based on NMR for the entire DMAA copolymer series (Table 2), it is found that X is largest for the lowest feedstock composition but decreases as the ratio of MAA/M1 increases. The number-average molecular weight, M_n, of the unimodal copolymers was estimated by gel permeation chromatography (GPC). The M_n results summarized in Table 2 show that the polymer size increases with the feedstock composition up to 3 and that larger polymers are formed at pH 6 than at pH 4 or 4.5 for a constant feedstock composition. These features indicate that control of polymer size depends upon a balance between feedstock composition and total ionic charge. On the basis of the protonation constants of M2, it is known that M1 will be positively charged with at least one proton associated with the macrocyclic N atoms at pH 6.0, and under these conditions most of the MAA is negatively charged. If the electrostatic attractions between positive and negative composition monomers are equal during the free radical propagation step, then one would anticipate production of larger polymers. Indeed, DMAA 3.1 had the highest molecular weight (58 500 Da) and degree of copolymerization ($Y = 58.9$). This degree of polymerization is about 5 times greater than that of homopolymer, H1, prepared using similar experimental conditions.[29]

Table 3 compares similar data (feedstock ratios, experimental condition, and characterization) for the DAMPS copolymers. The correlation between the resulting copolymer size and experimental condition follows a similar trend as observed for DMAA. Again, the copolymer displaying the highest degree of copolymerization ($Y = 20.1$) was DAMPS 3.1, but in this case, the number-average molecular weight was about 2-fold smaller.

NIPAM containing copolymers typically exhibit LCST behavior such that raising the temperature of aqueous polymer solutions above a certain critical temperature results in phase separation.[33] This feature proved to be a problem for syntheses of DNIPAM copolymers in aqueous solution because phase separation occurred upon initiation of the copolymerization reactions at 70 °C. For this reason, the solvent was switched to DMF for this reaction. However, the DNIPAM copolymers produced in DMF had lower molecular weights and degrees of copolymerization (Table 4) compared to the DMAA and DAMPS copolymers prepared in an aqueous medium. The composition of these polymers paralleled the initial feedstock composition (at least for these two values), and the molecular weights also increased with feedstock composition.

C. PARACEST Contrast Sensitivity Enhancement. The Eu^{3+} complexes were prepared by reacting excess $Eu(OTf)_3$ with each polymer in H_2O at pH 6.0 with stirring for several days. Nitrilotriacetate was added to sequester any free Eu^{3+}, and the resulting Eu-heteropolymers were purified by dialysis using 3000 MW cutoff tubing. It is known that the EuDOTA-tetraamide complexes such as this exist in solution as a mixture of two coordination isomers: a monocapped square antiprism (SAP) and a twisted monocapped square antiprism (TSAP) structure.[34] SAP isomers typically display much slower water exchange ($k_{ex} = 1/\tau_M$) compared to TSAP isomers[35] so it is most favorable for CEST if these complexes exist in solution largely or exclusively as the SAP coordination isomer. The isomer population was measured directly by ^{1}H NMR as illustrated

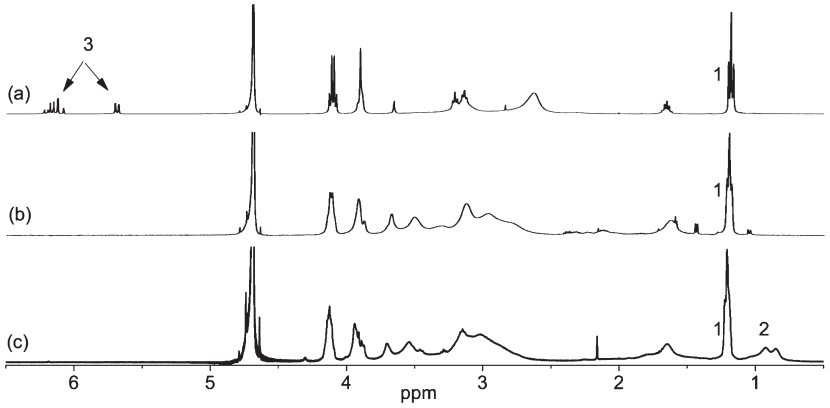

Figure 1. ^{1}H NMR spectra of (a) monomer M1, (b) homopolymer H1, and (c) copolymer DMAA 2.1 in D_2O. Peaks 1 and 2 assigned to the methyl protons of M1 and MAA units, respectively, and peak 3 to the protons on carbon−carbon double bond.

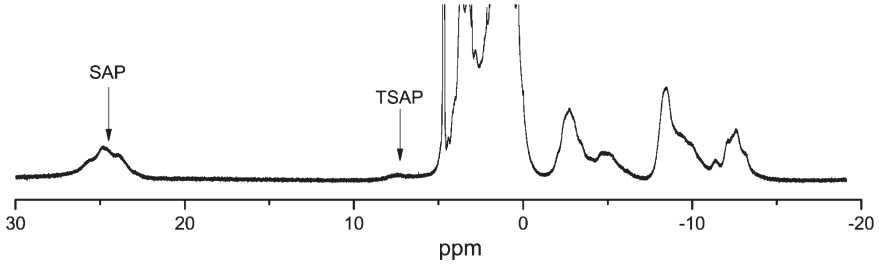

Figure 2. ^{1}H NMR spectrum of Eu-DMAA 2.1 in D_2O. The arrows point to resonances typical of the macrocyclic H_4 proton resonances in EuDOTA-tetraamide complexes existing in either a square antiprism (SAP) or twisted square antiprism (TSAP) coordination geometry.

by the spectrum of Eu-DMAA 2.1 in Figure 2. The largest peaks between 0.5 and ~4.5 ppm can be ascribed to unshifted protons in the polymer backbone, MAA methyl groups, and M1 ethyl ester groups while the remaining more highly shifted resonances arise from protons position near the Eu-M1 subunits. For analogous EuDOTA-tetraamide complexes, the axial macrocyclic protons of a SAP isomer typically appears around 24−36 ppm while the corresponding axial protons in a TSAP isomer are found in the 5−12 ppm range.[36] Eu-DMAA 2.1 also displays a set of SAP axial proton resonances near 22−27 ppm and a less intense group of resonances between 6 and 8 ppm. From the ratio of these two groups of resonances, one finds that the EuDOTA-tetraamide complexes in this polymer exist largely as the SAP isomer (95:5 by NMR integration). Similar results were observed in ^{1}H NMR spectra of the other Eu-copolymer complexes as well. This suggests that the Eu^{3+} coordination geometry in the M1 component is largely unaffected by the other copolymer component. In addition, the integration of the unshifted protons (0.5−4.5 ppm) closely matches the copolymer composition, so one can conclude that the majority of macrocyclic ligand sites in these polymers were occupied by Eu^{3+}.

To evaluate the CEST efficiency and water exchange properties of these Eu-copolymers, CEST spectra of Eu-M1 and Eu-DMAA 2.1 were measured under identical conditions (Figure 3). The resulting CEST profiles of Eu-M1 and Eu-DMAA 2.1 were essentially identical with respect to CEST efficiencies ($1 - M_S/M_0$) on a per Eu^{3+} basis. No CEST signal was evident after presaturation in the region of the spectra where the coordinated water molecules of the TSAP isomers resonate (10−20 ppm), indicating that water exchange is too fast to detect CEST from this isomer, as expected. The CEST spectra were fit to a three-pool exchange model based upon the modified Bloch equations[37] in which water exchange is considered only from SAP isomer. This fitting afforded water residence lifetimes (τ_M) of 149 ± 16 μs for Eu-M1 and 164 ± 18 μs for Eu-DMAA 2.1 (Table 5). This indicates that water

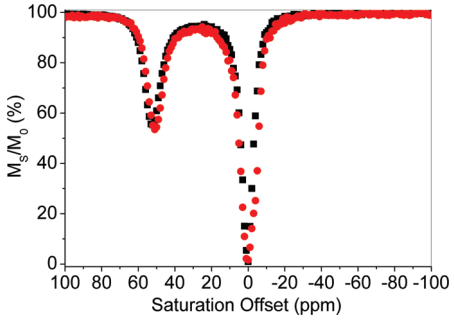

Figure 3. CEST spectra of Eu-M1 (●) and Eu-DMAA 2.1 (■) recorded at 9.4 T, 25 °C, and neutral pH. [Eu^{3+}] = 30 mM, B_1 = 14.1 μT, saturation time = 2 s.

exchange is essentially unimpeded by formation of the copolymer between MAA and M1. The remaining CEST spectra and water exchange lifetimes of the other Eu^{3+}-polymers are reported in Figures S1a−S1m and Table 5, respectively. It is interesting to note for the Eu-DMAA series that τ_M decreases (water exchange rate increases) with an increase in MAA subunit composition. Conversely, the Eu-DAMPS and Eu-DNIPAM copolymers do not show a significant sensitivity of τ_M to polymer composition at 25 °C.

Although formation of copolymers consisting of M1 and one of three other acrylamide components appears not to have a dramatic effect on the Eu^{3+}-bound water exchange rates and the CEST effect on a per Eu^{3+} basis, the potential utility of these systems as a platform for increasing the effective local concentration of a targeted PARACEST agent remains interesting. A plot of CEST intensity ($1 - M_S/M_0$) versus the average agent concentration or polymer concentration of various Eu-DMAA copolymers is shown in Figure 4 (similar data can be found for Eu-DAMPS and Eu-DNIPAM in Figure S2). In comparison with the Eu-M1

Table 5. pH Dependence of CEST Fitting Results of τ_M (ms) and δ (ppm) of Bound Water and CEST Efficiency for Various Complexes Recorded at 9.4 T and 25 °C ([Eu^{3+}] = 30 mM and Satuaration Time = 2 s)

complexes	pH	τ_M (ms)	δ (ppm)	$1 - M_S/M_0$ (%)
Eu-M1	6.8	0.149 ± 0.001	51.9 ± 0.1	49
Eu-DMAA 1.1	7.6	0.179 ± 0.004	52.0 ± 0.1	52
	4.1	0.141 ± 0.003	49.5 ± 0.1	43
Eu-DMAA 2.0	6.6	0.143 ± 0.003	52.0 ± 0.2	48
	4.2	0.117 ± 0.012	51.4 ± 0.1	36
Eu-DMAA 2.1	6.6	0.164 ± 0.018	52.1 ± 0.4	45
	4.3	0.120 ± 0.010	51.8 ± 0.2	37
Eu-DMAA 3.0	7.5	0.147 ± 0.007	54.0 ± 0.1	49
	4.2	0.092 ± 0.004	53.8 ± 0.1	39
Eu-DMAA 3.1	7.0	0.143 ± 0.006	53.2 ± 0.1	53
	4.5	0.094 ± 0.006	51.6 ± 0.2	43
Eu-DMAA 4.1	6.7	0.109 ± 0.005	54.4 ± 0.1	46
Eu-DAMPS 1.1	6.7	0.150 ± 0.002	49.4 ± 0.2	59
	4.3	0.157 ± 0.004	48.8 ± 0.2	56
Eu-DAMPS 2.0	6.9	0.163 ± 0.009	48.7 ± 0.2	56
	4.2	0.180 ± 0.008	47.9 ± 0.2	54
Eu-DAMPS 2.1	7.5	0.158 ± 0.016	48.8 ± 0.1	54
	4.0	0.175 ± 0.003	48.0 ± 0.2	51
Eu-DAMPS 3.1	8.0	0.162 ± 0.007	49.2 ± 0.1	46
	4.3	0.178 ± 0.002	48.4 ± 0.1	42
Eu-DAMPS 4.1	7.7	0.165 ± 0.017	51.2 ± 0.1	47
	4.5	0.175 ± 0.011	50.9 ± 0.1	45
Eu-DNIPAM 3.0	7.3	0.161 ± 0.026	49.1 ± 0.2	41
Eu- DNIPAM 4.0	6.8	0.148 ± 0.003	50.5 ± 0.1	48

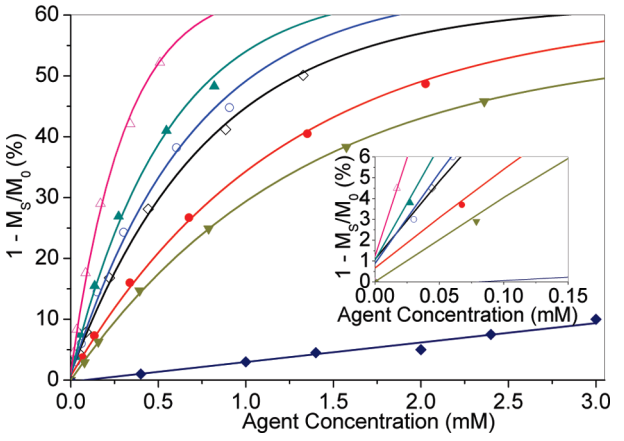

Figure 4. Plot of CEST intensity ($1 - M_S/M_0$) as a function of concentration for various Eu-DMAA copolymers (1.1 ◇, 2.0 ●, 2.1 ○, 3.0 ▲, 3.1 △, and 4.1 ▼) or Eu-M1 (◆) recorded at 9.4 T, 25 °C, and neutral pH (B_1 = 14.1 μT and saturation time = 2 s). Symbols: experimental data. Lines: fitted data to an exponential decay. Inset: amplified view showing the plot near the 5% threshold for CEST detection.

monomer, the polymeric agents display a sharp increase in CEST sensitivity with increasing degree of copolymerization as anticipated. The detection limit of each agent, based on the assumption that a 5% CEST effect is the minimum amount needed for detection, ranges from 20 to 610 μM, significantly lower than that of the Eu-M1 monomer (1650 ± 160 μM) (Table 6). In particular, the detection limit found for Eu-DMAA 3.1 (20 ± 2 μM) is 6.5 times lower than that measured for homopolymer, Eu−H1 (130 ± 6 μM), prepared under similar polymerization condition.[29] This demonstrates that a significant improvement in CEST contrast sensitivity can be further achieved by preparing even higher molecular weight copolymer scaffolds.

D. Affects of Random Copolymer Variations on Polymer Performance and CEST Properties. As indicated above, the number of CEST units in each polymer plays a much bigger role in amplification of CEST contrast sensitivity than does

Table 6. Detection Limits[a] for Polymeric CEST Agents at 25 °C Using B_1 = 14.1 μT

complexes	(μM)[a]	complexes	(μM)
Eu-DMAA 1.1	54 ± 3	Eu-DAMPS 1.1	71 ± 10
Eu-DMAA 2.0	93 ± 3	Eu-DAMPS 2.0	60 ± 5
Eu-DMAA 2.1	49 ± 1	Eu-DAMPS 2.1	75 ± 2
Eu-DMAA 3.0	37 ± 1	Eu-DAMPS 3.1	99 ± 7
Eu-DMAA 3.1	20 ± 2	Eu-DNIPAM 3.1	610 ± 30
Eu-DMAA 4.1	124 ± 3	Eu-DNIPAM 4.1	470 ± 10
Eu-M1	1650 ± 160		

[a] These detection limits were determined using a single rf power (B_1 = 14.1 μT). One could reach even lower detection limits by use of higher power presaturation pulses, but the variation in detection limits for the various polymers should be similar as those shown here.

changes in τ_M. This is in contrast to the small monomer complexes where τ_M is the major parameter that controls CEST sensitivity.[6,7] Despite the small role played by τ_M in controlling the CEST contrast sensitivity in polymeric agents, it is still worthwhile to investigate the polymer composition variation dependence of τ_M. Such studies are useful for developing an understanding of the fundamental aspects that affect τ_M and, consequently, the CEST properties.

Analogous to the pH-induced hydrophilicity changes in pH-responsive poly(methacrylic acid),[33] the hydrophilicity of DMAA-based agents can be regulated by the proportion of MAA subunits and hydrophobicity can be varied in the DNIPAM-based agents by changing the proportion of NIPAM subunits. This makes it possible to investigate the composition variations dependence of τ_M for the polymeric complexes.

Light scattering experiments were carried out to assess the sensitivity of polymer solubility and composition to pH and temperature variations. Solutions of Eu-DMAA 4.1 showed a sharp pH-responsive behavior, turning from clear to turbid, as the pH dropped below 4.8 (Figure 5a). Interestingly, this same behavior was not observed for Eu-DMAA 3.1 (Figure 5a) and the remaining Eu-DMAA complexes. This physical behavior approximately parallels protonation of the carboxylate groups in the MAA subunits of Eu-DMAA 4.1, resulting in a sharp transition from water-soluble to insoluble near pH ~4.7−4.8. The copolymer DNIPAM 4.0 (metal ion free) and its Eu^{3+} complex showed thermoresponsive behavior (Figure 5b). Here, solutions of DNIPAM 4.0 were transparent below 32 °C but completely turbid above 40 °C where the efficiency of hydrogen bonding between the NIPAM units and water becomes reduced. The LCST estimated from the first derivative of this curve (35 °C) is ~3 °C higher than that of PNIPAM.[33] Addition of Eu^{3+} to the polymer to form Eu-DNIPAM 4.0 resulted in a shift in LCST to a higher temperature (43 °C), presumably due to the extra charge introduced into the polymer by the Eu^{3+}. It is also interesting that the phase transition in Eu-DNIPAM 4.0 is quite different from that of Eu-DMAA 4.1. In the latter system, the phase transition is characterized by the polymer precipitation from the aqueous solution while Eu-DNIPAM 4.0 remains suspended in solution above the LCST for at least several hours.

These results suggest that the multifunctional polymeric scaffolds have new properties that may be conducive to applications other than CEST imaging agents. The responsive behavior of polymers can be attributed to the incremental variations in polarity versus hydrophobicity in response to changes in pH and temperature which, in turn, will likely affect the CEST properties of these systems. Not surprisingly, large changes in CEST were observed for Eu-DMAA 4.1 as the polymer precipitated from solution below pH ~4.7 (Figure S5a). In comparison, less than a 4% change in CEST was observed with similar changes in pH for the Eu-DAMPS polymer series on Eu^{3+} basis (Figure S5b and Table 5). This difference is partially attributed to the fact that the Eu-DAMPS systems do not

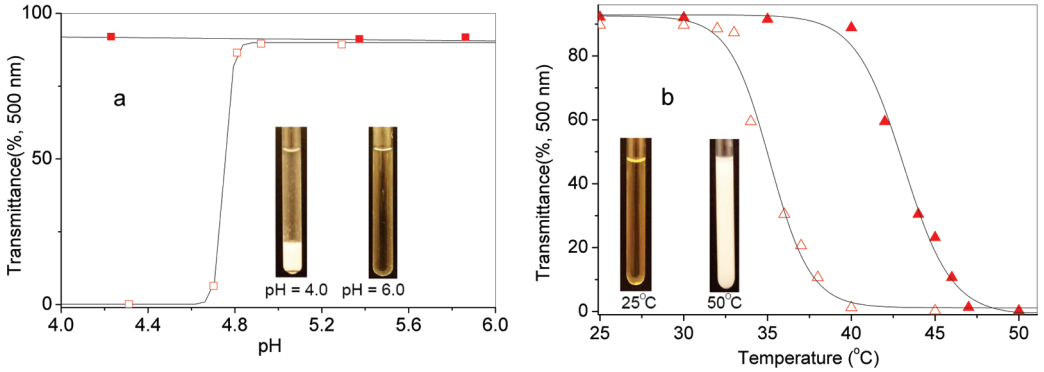

Figure 5. (a) Comparison of light scattering as a function of pH for samples of Eu-DMAA 3.1 (■) and Eu-DMAA 4.1 (□) (2 wt %) in aqueous solutions at 25 °C. Inset: photographs of an aqueous solution Eu-DMAA 4.1 at pH 4.0 and 6.0, respectively. (b) Comparison of light scattering as a function of temperature for samples of DNIPAM 4.0 (△) and Eu-DNIPAM 4.0 (▲) (2 wt %) in neutral aqueous solution. Inset: photographs of Eu-DNIPAM 4.0 in aqueous solution at 25 and 50 °C, respectively. Symbols: experimental data. Lines: fitted data to simple sigmoidal function.

undergo a change in overall charge over this same pH range.[8,9] For the remaining Eu-DMAA complexes (those that do not precipitate at low pH), a slight decrease in CEST of 8−12% (per Eu^{3+}) was found as the pH was lowered from 8 to 4. This can be attributed to a decrease in τ_M (30−50 μs) that occurs over this same pH range (Table 5). Given that the mechanism of water exchange in such complexes is thought to be largely dissociative,[38] relative to the carboxylate group, the carboxylic acid group in Eu-DMAA at low pH forms stronger hydrogen bond with the surrounding water,[39] and this promotes access of more bulk water into the polymer and enhances water exchange at each local Eu^{3+} site along the polymer backbone. For the Eu-DAMPS series, however, the AMPS subunits are not protonated over this same pH range (due to the low pK_a value of sulfonate groups) so water accessibility to the Eu^{3+} centers in Eu-DAMPS remains essentially insensitive to pH.

The dramatic polarity differences observed in Eu-DNIPAM 4.0 and Eu-DMAA 4.1 promoted further studies to gain more insight into the relationship between the composition variations and τ_M. The CEST spectra of Eu-DNIPAM 4.0, Eu-DMAA 4.1, and Eu-M1 measured as a function of temperature (shown in Figure 6) revealed insight into the relationship between the CEST signal and water exchange in the monomer and polymer series. The Eu^{3+}-bound water exchange peak in Eu-DNIPAM 4.0 increased in intensity from 25 to 30 °C and then gradually decreased in intensity, broadened, and shifted toward the bulk water peak as the temperature was further increased (Figure 6a). Except for the absolute magnitude of CEST, which is higher for Eu-DNIPAM 4.0 at each temperature, the temperature curves for all three samples were qualitatively similar (Figure 6). The temperature-dependent profiles for Eu-DMAA 4.1 differ from the other two in that CEST is largest at 25 °C and drops off rapidly with an increase in temperature (Figure 6b).

The τ_M values derived from each of these CEST profiles are plotted as a function of temperature in Figure 7. Hydrogen bonding between the water and NIPAM subunits in Eu-DNIPAM 4.0 is weaker at the higher temperatures so the NIPAM subunits tend to associate more with each other. This hinders access of entering water molecules and water exchange from the Eu^{3+} sites becomes slower (Figure 7). In comparison, the carboxylate groups in the MAA subunits of Eu-DMAA 4.1 are good hydrogen-bonding acceptors, and this favors formation of a hydrogen bond network with bulk water surrounding the polymer. This allows more water molecules to have immediate access to each Eu^{3+} center, and consequently water exchange is accelerated (Figure 7). It was reported for EuDOTA-tetraamide complexes that the bound water lifetimes increase with decreasing

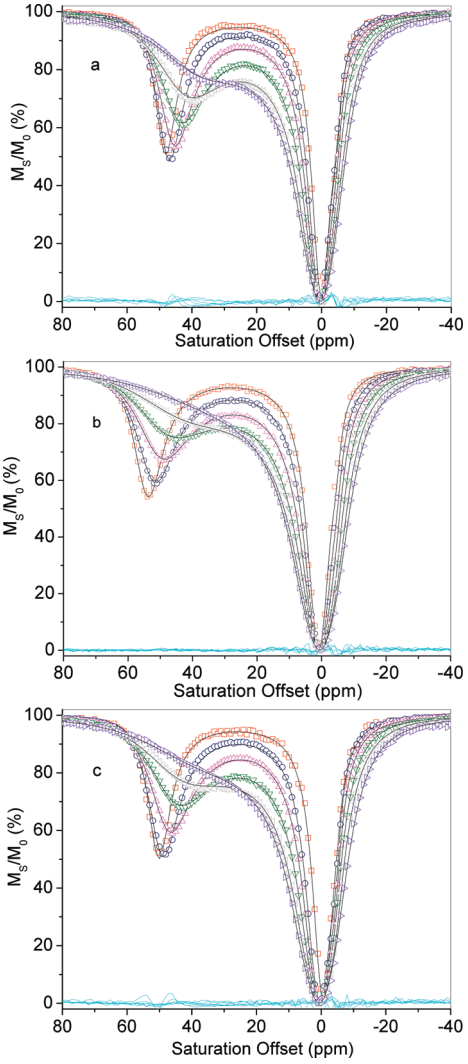

Figure 6. Temperature (25 °C □, 30 °C ○, 35 °C △, 40 °C ▽, 45 °C left-pointing △, and 50 °C right-pointing △) dependence of CEST spectra of (a) Eu-DNIPAM 4.0, (b) Eu-DMAA 4.1, and (c) Eu-M1 recorded around pH 7 at 9.4 T. [Eu^{3+}] = 30 mM, B_1 = 14.1 μT, saturation time = 2 s. Symbols: experimental data. Lines: the result of fitting these data to the Bloch equations.

polarity in the ligand side chains.[38] In the case of the copolymers reported herein, the bound water lifetimes increase with decreasing hydrophilicity of the polymer

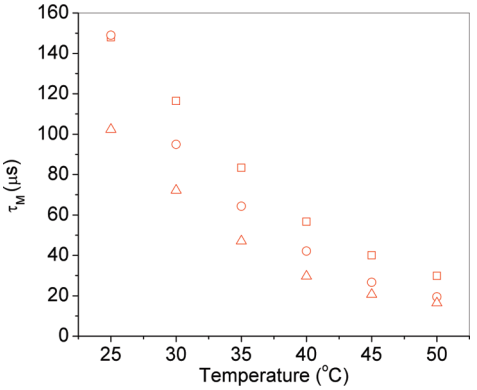

Figure 7. Temperature dependence of water residence lifetime for Eu-M1 (○), Eu-DMAA 4.1 (△), and Eu-DNIPAM 4.0 (□) recorded around pH 7 at 9.4 T. [Eu^{3+}] = 30 mM, B_1 = 14.1 μT, saturation time = 2 s.

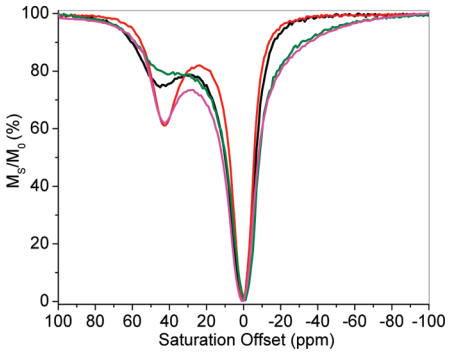

Figure 8. CEST spectra of Eu-DMAA 4.1 (black) and Eu-NIPAM 4.0 (red) recorded in water versus plasma (Eu-DMAA 4.1 (green) and Eu-NIPAM 4.0 (pink)). All samples were recorded at 40 °C and 9.4 T at neutral pH. [Eu^{3+}] = 30 mM, B_1 = 14.1 μT, saturation time = 2 s.

compositions. These observations will be useful for predicting further ways to improve the efficiency of polymeric PARACEST agents for imaging applications.

E. Performance of the CEST Polymers in Serum. The CEST properties of these polymers in plasma were examined to test their properties *in vivo*. It was found, on a per Eu^{3+} basis, that CEST is similar for Eu-DNIPAM 4.0 but somewhat lower for Eu-DMAA 4.1 when dissolved in plasma compared to these same systems dissolved in water at 25 and 40 °C (Figure 8 and Figure S6). This result suggests that the more hydrophilic polymer, Eu-DMAA 4.1, interacts with plasma proteins likely through ion pairing interactions, and this catalyzes faster water exchange at the Eu^{3+} sites in the polymer leading to a quenching of its CEST properties. Conversely, the CEST properties of more hydrophobic polymer, Eu-DNIPAM 4.0, are largely unaltered by plasma proteins, indicating that water exchange in this system remains essentially unaltered. This does not discount possible binding interactions between the polymer and the protein but does indicate that water exchange and the resulting CEST signal should remain unaltered when used *in vivo*.

Conclusions

We have developed a convenient methodology for preparing of a series of multifunctional copolymer PARACEST agents for potential use as imaging agents *in vivo*. Some of the solution properties of the heteropolymers changed quite dramatically with changes in pH and temperature, leading to the possibility of using them as reporters of physiological parameters *in vivo*. Furthermore, heteropolymers containing a large fraction of hydrophobic components appear to be most advantageous for *in vivo* CEST applications.

Experimental Section

A. General. All reagents and solvents were purchased from commercially available sources and used as received unless otherwise stated. ^1H and ^{13}C NMR spectra were recorded on a Bruker AVANCE III 400 NMR spectrometer operating at 400.13 and 100.62 MHz, respectively. CEST spectra were recorded on the same NMR spectrometer operating at 400.13 MHz. Presaturation pulses of 2 s duration were applied at four saturation powers of 9.4, 14.1, 18.8, and 23.5 μT. The CEST spectra were fitted to the Bloch equations with three-pool model by use of a nonlinear fitting algorithm written in MATLAB 7 (Mathworks Inc., Natick, MA).[37] Specifically, the basic experimental parameters such as T_1 and T_2 of bulk water, presaturation times, saturation powers, and proton concentrations of bulk water, bound water, and amides were used as prior information in a MATLAB program used to fit to the individual experimental CEST spectrum. These fittings gave values for τ_M of the bound water and amide protons, the $\Delta\omega$ values for bulk water, bound water and the amide protons, and the T_1 and T_2 of the bound water and the amide protons. The bound water τ_M values were reported as the mean based on spectra collected using four different power levels for each sample.

The agents were dissolved either in pure water or in human plasma containing NaEDTA (Innovative Research, Novi, MI) for CEST measurements. The Eu^{3+} concentrations of the stock polymeric agents were determined via inductively coupled plasma mass spectrometry (ICP MS). The volume of each polymer stock solution was diluted or concentrated to an appropriate level necessary to obtain high-quality CEST spectra. The polymeric agent concentrations used in section C for the sensitivity studies were calculated from the above quantitative Eu^{3+} concentration by dividing the degree of polymerization relative to the DOTA monomer unit with the assumption that every DOTA chelate contained a Eu^{3+} ion.

The pH potentiometry titrations were carried out using established methods[30] and performed on Metrohm titration system with a Thermo EA940 pH meter. The protonation constants (log K_i^H) and stability constants of the complexes (log K_{ML}) were evaluated based on the potentiometric titration data using the program PSEQUAD.[40] The log K_{ML} were calculated from the data obtained over the pH range 2.9−12.0 for Ca^{2+} and Mg^{2+} complexes, 1.8−12.0 for Zn^{2+} and Cu^{2+} complexes, and 2.6−5.6 for Eu^{3+} complexes.

Molecular weights of copolymers were determined with Viscogel columns (GMHHR-M type) on GPC system equipped with Viscotek VE 3580 RI detector. DMF was used as eluent with a flow rate of 1 mL/min. A series of poly(methyl methacrylate) standards were employed for instrument calibration. The pH and thermoresponse of the polymers in aqueous solutions were determined spectrophotometrically using a Varian Cary 300 Bio UV/vis spectrophotometer equipped with a thermostated cell holder. The polymer concentrations were always maintained at 2 wt %, and the transmittance at 500 nm was measured.

B. Synthesis. M1 and M2 were prepared by using established procedures.[29]

General Procedure for the Synthesis of DMAA and DAMPS Copolymers. Taking the preparation of DMAA 2.1 as an example. Water (4 mL), M1 (120 mg, 0.16 mmol), 2-methylacrylic acid (13 μL, 0.16 mmol), and 4,4′-azobis(4-cyanovaleric acid) (12 mg, 0.04 mmol) were introduced into a 10 mL round-bottom flask and stirred at room temperature to give a homogeneous solution. The reaction mixtures were then adjusted to pH 6.0 by careful addition of NaOH, and the N_2 was slowly bubbled through solution for 30 min to remove dissolved oxygen. The reaction solution was heated under N_2 at 70 °C

for 24 h. The reaction mixtures were then cooled to room temperature and filtered. The resulting copolymer was purified by dialysis using 3000 MW cutoff dialysis tubing and lyophilized to dryness giving the copolymer as white powder. ^{1}H NMR (400 MHz, D_2O), δ 4.11−4.14 (6H, m br, OCH_2CH_3), 3.87−3.94 (6H, m br, $NHCH_2CO_2$), 2.85−3.70 (28H, m br, $NCH_2C{=}O$, $CH_2CH_2CH_2$ and ring CH_2N), 1.64−1.78 (7H, d br, CH_2CH_2-CH_2 and polymer backbone), 1.21 (9H, t br, CH_2CH_3), 0.85−0.92 (3.7 H, d br, CCH_3). ^{13}C NMR (100 MHz, D_2O): δ 183.6 (s br, C=O), 175.8 (s br, C=O), 171.2 (s br, C=O), 62.5 (s br, OCH_2CH_3), 56.0 (s br, $NHCH_2CO_2$), 49.9 (s br, ring CH_2N), 46.3 (s br, polymer backbone), 43.3 (s br, $NCH_2C{=}O$), 41.3 (s br, $NCH_2C{=}O$), 37.1 (m br, $CH_2CH_2CH_2$, $CH_2CH_2CH_2$), 28.5 (d br, $CH_2CH_2CH_2$), 19.8 (s br, CH_3CH) 18.3 (s br, CH_3CH), 13.4 (d br, CH_3CH_2O).

General Procedure for the Synthesis of DNIPAM Copolymers. Taking the preparation of DNIPAM 4.0 as an example. DMF (4 mL), M1 (120 mg, 0.16 mmol), *N*-isopropylacrylamide (163 mg, 1.44 mmol), and 4,4′-azobis(4-cyanovaleric acid) (12 mg, 0.04 mmol) were introduced into a 10 mL round-bottom flask and stirred at room temperature to give a homogeneous solution. The N_2 was slowly bubbled through solution for 30 min to remove dissolved oxygen. The reaction solution was heated under N_2 at 70 °C for 24 h. The reaction mixtures were then cooled to room temperature, and DMF was removed under vacuum to give a pale yellow solid, which was dissolved in water and filtered. The resulting copolymer was purified by dialysis using 3000 MW cutoff dialysis tubing and lyophilized to dryness giving the DNIPAM 4.0 as white powder. ^{1}H NMR (400 MHz, D_2O): δ 4.10−4.12 (6H, m br, OCH_2CH_3), 3.81−3.89 (m br, $NHCH_2CO_2$ and CH), 2.71−3.47 (m br, $NCH_2C{=}O$, $CH_2CH_2CH_2$ and ring CH_2N), 1.93−2.04 (d br, polymer backbone), 1.42−1.60 (m br, CH_2CH_2-CH_2 and polymer backbone), 1.18 (9H, s br, CH_2CH_3), 1.06 (55 H, s br, CCH_3). ^{13}C NMR (100 MHz, D_2O): δ 175.3 (s br, C=O), 173.9 (s br, C=O), 171.1 (s br, C=O), 62.5 (s br, OCH_2CH_3), 56.4−57.3 (m br, $NHCH_2CO_2$), 50.2 (m br, ring CH_2N), 42.3 (s br, $NCH_2C{=}O$), 41.3−42.1 (s br, $NCH_2C{=}O$ and CH), 30.2−36.9 (m br, $CH_2CH_2CH_2$, $CH_2CH_2CH_2$ and polymer backbone), 28.5 (s br, $CH_2CH_2CH_2$), 21.5 (s br, CH_3CHCH_3), 13.4 (s br, CH_3CH_2O).

General Procedure for the Synthesis of Eu-Copolymer Complexes. Taking the preparation of Eu-DMMA 2.1 as an example. DMMA 2.1 (28 mg, 0.031 mmol of the corresponding M1 subunit) and europium triflate (22 mg, 0.036 mmol) were dissolved in water (3.0 mL). The mixture was adjusted to a pH around 6.0 by careful addition of NaOH. The pH of reaction mixture was maintained at around 6.0 and stirred at room temperature for a week. If free Eu^{3+} was detected at this point by use of xylenol orange, the solution is filtered, and the resulting Eu-polymer complexes were purified by dialysis using 3000 MW cutoff dialysis tubing. If a second xylenol orange test indicates free Eu^{3+} is still present, nitrilotriacetate (0.004 mmol) was then added to chelate excess Eu^{3+}, and the dialysis repeated. If no free Eu^{3+} was detected at this point, the aqueous solution was filtrated and lyophilized to give the complex as white powder. ^{1}H NMR (400 MHz, D_2O): δ 23.5−24.7 (t br), 7.4 (s br), 0.3−3.7 (m br), −2.7 (s br), −4.8 (s br), −8.3 (s br), −11.3 to −12.5 (m br).

Procedure for the Synthesis of Eu-DMAA 4.1 Complexes. Precipitation was observed during preparation of the Eu-DMAA 4.1 likely due to rapid binding of Eu^{3+} to the carboxylate anions of the polymer, similar to that seen during preparation of humic acid−M^{3+} complexes.[41] To circumvent this problem, a competitive binding method was used to prevent precipitation of the polymer. Europium triflate (22 mg, 0.036 mmol) and sodium citrate (9.3 mg, 0.036 mmol) were dissolved in water (2.0 mL), and the pH of the mixture was adjusted to ~6.0 by addition of NaOH. This solution was added slowly to a solution of DMAA 4.1 (1 mL, 0.032 mmol of the corresponding M1 subunit and pH = 6.0), thereby circumventing the precipitation problem. The pH of resulting reaction mixture was maintained near 6.0 and stirred at room temperature for a week. The resulting Eu-polymer complexes were purified by dialysis using 3000 MW cutoff dialysis tubing. If the resulting solution tested positive for free Eu^{3+}, nitrilotriacetate (0.004 mmol) was added and the dialysis was repeated. When the sample contained no free Eu^{3+}, the aqueous solution is filtrated and lyophilized to give the complex as white powder. ^{1}H NMR (400 MHz, D_2O): δ 24.9−25.2 (d br), 7.5 (s br), 0.9−3.3 (m br), −2.6 (d br), −4.8 to −6.0 (d br), −8.2 (s br), −9.9 to −10.5 (d br), −12.0 to −13.0 (s br).

Acknowledgment. The authors thank Dr. Gyula Tircsó (University of Debrecen) for his assistance with the pH-potentiometric studies and thank Drs. Mihaela C. Stefan and Mussie G. Alemseghed (University of Texas at Dallas) for their assistance with the GPC molecular weight measurements. Financial support from the National Institutes of Health (CA115531, RR02584, and EB004582) and the Robert A. Welch Foundation (AT-584) is gratefully acknowledged.

Supporting Information Available: Proton constant data; CEST fitting spectra; pH dependence of transmittance spectra for Eu-DMAA 4.1; temperature dependence of transmittance spectra for DNIPAM 4.0 and Eu-DNIPAM 4.0; pH dependence of CEST spectra for Eu-DMAA 4.1 and Eu-DAMPS 4.1; temperature dependence of CEST spectra for Eu-DNIPAM 4.0 and Eu-DMAA 4.1 in plasma. This material is available free of charge via the Internet at http://pubs.acs.org.

References and Notes

(1) Caravan, P.; Ellison, J. J.; McMurry, T. J.; Lauffer, R. B. *Chem. Rev.* **1999**, *99*, 2293–2352.
(2) *The Chemistry of Contrast Agents in Medical Magnetic Resonance Imaging*; Merbach, A. E., Toth, E., Eds.; John Wiley & Son: Chichester, UK, 2001.
(3) *Molecular and Cellular MR Imaging*; Modo, M., Bulte, J., Eds.; CRC Press Taylor & Francis Group: Boca Raton, FL, 2007.
(4) Sherry, A. D.; Woods, M. *Annu. Rev. Biomed. Eng.* **2008**, *10*, 391–411.
(5) Zhou, J. Y.; van Zijl, P. C. M. *Prog. Nucl. Magn. Reson. Spectrosc.* **2006**, *48*, 109–136.
(6) Zhang, S. R.; Merritt, M.; Woessner, D. E.; Lenkinski, R. E.; Sherry, A. D. *Acc. Chem. Res.* **2003**, *36*, 783–790.
(7) Woods, M.; Woessner, D. E.; Sherry, A. D. *Chem. Soc. Rev.* **2006**, *35*, 500–511.
(8) Aime, S.; Delli Castelli, D.; Terreno, E. *Angew. Chem., Int. Ed.* **2002**, *41*, 4334–4336.
(9) Aime, S.; Barge, A.; Castelli, D. D.; Fedeli, F.; Mortillaro, A.; Nielsen, F. U.; Terreno, E. *Magn. Reson. Med.* **2002**, *47*, 639–648.
(10) Terreno, E.; Castelli, D. D.; Cravotto, G.; Milone, L.; Aime, S. *Invest. Radiol.* **2004**, *39*, 235–243.
(11) Pikkemaat, J. A.; Wegh, R. T.; Lamerichs, R.; van de Molengraaf, R. A.; Langereis, S.; Burdinski, D.; Raymond, A. Y. F.; Janssen, H. M.; de Waal, B. F. M.; Willard, N. P.; Meijer, E. W.; Grull, H. *Contrast Media Mol. Imaging* **2007**, *2*, 229–239.
(12) Zhang, S. R.; Malloy, C. R.; Sherry, A. D. *J. Am. Chem. Soc.* **2005**, *127*, 17572–17573.
(13) Li, A. X.; Wojciechowski, F.; Suchy, M.; Jones, C. K.; Hudson, R. H. E.; Merton, R. S.; Bartha, R. *Magn. Reson. Med.* **2008**, *59*, 374–381.
(14) Trokowski, R.; Ren, J. M.; Kalman, F. K.; Sherry, A. D. *Angew. Chem., Int. Ed.* **2005**, *44*, 6920–6923.
(15) Zhang, S. R.; Trokowski, R.; Sherry, A. D. *J. Am. Chem. Soc.* **2003**, *125*, 15288–15289.
(16) Trokowski, R.; Zhang, S. R.; Sherry, A. D. *Bioconjugate Chem.* **2004**, *15*, 1431–1440.
(17) Ren, J. M.; Trokowski, R.; Zhang, S. R.; Malloy, C. R.; Sherry, A. D. *Magn. Reson. Med.* **2008**, *60*, 1047–1055.
(18) Aime, S.; Delli Castelli, D.; Fedeli, F.; Terreno, E. *J. Am. Chem. Soc.* **2002**, *124*, 9364–9365.
(19) Liu, G. S.; Li, Y. G.; Pagel, M. D. *Magn. Reson. Med.* **2007**, *58*, 1249–1256.
(20) Huang, C. H.; Morrow, J. R. *J. Am. Chem. Soc.* **2009**, *131*, 4206–4207.
(21) Yoo, B.; Pagel, M. D. *J. Am. Chem. Soc.* **2006**, *128*, 14032–14033.
(22) Yoo, B.; Raam, M. S.; Rosenblum, R. M.; Pagel, M. D. *Contrast Media Mol. Imaging* **2007**, *2*, 189–198.

(23) Chauvin, T.; Durand, P.; Bernier, M.; Meudal, H.; Doan, B. T.; Noury, F.; Badet, B.; Beloeil, J. C.; Toth, E. *Angew. Chem., Int. Ed.* **2008**, *47*, 4370–4372.
(24) Kobayashi, H.; Brechbiel, M. W. *Curr. Pharm. Biotechnol.* **2004**, *5*, 539–549.
(25) Kim, J. H.; Park, K.; Nam, H. Y.; Lee, S.; Kim, K.; Kwon, I. C. *Prog. Polym. Sci.* **2007**, *32*, 1031–1053.
(26) Lanza, G. M.; Winter, P. M.; Caruthers, S. D.; Morawski, A. M.; Schmieder, A. H.; Crowder, K. C.; Wickline, S. A. *J. Nucl. Cardiol.* **2004**, *11*, 733–743.
(27) Goffeney, N.; Bulte, J. W. M.; Duyn, J.; Bryant, L. H.; van Zijl, P. C. M. *J. Am. Chem. Soc.* **2001**, *123*, 8628–8629.
(28) Aime, S.; Delli Castelli, D.; Terreno, E. *Angew. Chem., Int. Ed.* **2003**, *42*, 4527–4529.
(29) Wu, Y. K.; Zhou, Y. F.; Ouari, O.; Woods, M.; Zhao, P. Y.; Soesbe, T. C.; Kiefer, G. E.; Sherry, A. D. *J. Am. Chem. Soc.* **2008**, *130*, 13854–13855.
(30) Pasha, A.; Tircso, G.; Benyo, E. T.; Brucher, E.; Sherry, A. D. *Eur. J. Inorg. Chem.* **2007**, 4340–4349.
(31) Baranyai, Z.; Brucher, E.; Ivanyi, T.; Kiraly, R.; Lazar, I.; Zekany, L. *Helv. Chim. Acta* **2005**, *88*, 604–617.
(32) Braun, D.; Cherdron, H.; Rehahn, M.; Ritter, H.; Voit, B. *Polymer Synthesis: Theory and Practice*; Springer: Berlin, 2005.
(33) Minko, S. *Responsive Polymer Materials: Design and Applications*; Wiley-Blackwell: Hoboken, NJ, 2006.
(34) Aime, S.; Barge, A.; Bruce, J. I.; Botta, M.; Howard, J. A. K.; Moloney, J. M.; Parker, D.; de Sousa, A. S.; Woods, M. *J. Am. Chem. Soc.* **1999**, *121*, 5762–5771.
(35) Dunand, F. A.; Aime, S.; Merbach, A. E. *J. Am. Chem. Soc.* **2000**, *122*, 1506–1512.
(36) Adair, C.; Woods, M.; Zhao, P. Y.; Pasha, A.; Winters, P. M.; Lanza, G. M.; Athey, P.; Sherry, A. D.; Kiefer, G. E. *Contrast Media Mol. Imaging* **2007**, *2*, 55–58.
(37) Woessner, D. E.; Zhang, S. R.; Merritt, M. E.; Sherry, A. D. *Magn. Reson. Med.* **2005**, *53*, 790–799.
(38) Aime, S.; Barge, A.; Batsanov, A. S.; Botta, M.; Castelli, D. D.; Fedeli, F.; Mortillaro, A.; Parker, D.; Puschmann, H. *Chem. Commun.* **2002**, 1120–1121.
(39) Jeffrey, G. A.; Saenger, W. *Hydrogen Bonding in Biological Structures*; Springer-Verlag: Berlin, 1991; pp 111−135.
(40) Zékány, L.; Nagypál, I. PSEQUAD: A Comprehensive Program for the Evaluation of Potentiometric and/or Spectrophotometric Equilibrium Data Using Analytical Derivatives. In *Computational Methods for Determination of Formation Constants*; Legett, D. J., Ed.; Plenum Press: New York, 1985; pp 291−353.
(41) Alfassi, Z. B. *J. Radioanal. Nucl. Chem.* **2004**, *262*, 77–81.